Damage Detection Methods on Wind Turbine Blade Testing with Wired and Wireless Accelerometer Sensors

Mark Mollineaux, Konstantinos Balafas, Kim Branner, Per Nielsen, Angelo Tesauro, Anne Kiremidjian, Ram Rajagopal

7th European Workshop on Structural Health Monitoring
July 8-11, 2014. La Cité, Nantes, France

DAMAGE DETECTION METHODS ON WIND TURBINE BLADE TESTING WITH WIRED AND WIRELESS ACCELEROMETER SENSORS

Mark Mollineaux[1], Konstantinos Balafas[2], Kim Branner[3], Per Nielsen[4], Angelo Tesauro[5], Anne Kiremidjian[6], Ram Rajagopal[7]

[1] *Stanford University*
[2] *Stanford University*
[3] *Technical University of Denmark Frederiksborgvej 399*
[4] *Technical University of Denmark Frederiksborgvej 399*
[5] *Technical University of Denmark Frederiksborgvej 399*
[6] *Stanford University*
[7] *Stanford University*

mgm1@stanford.edu

ABSTRACT

Testing was performed on a 34 meter blade at a facility in DTU Risø Campus, featuring both wired accelerometers and low-power MEMs-based wireless accelerometers. Testing was focused on an induced delamination area on the trailing edge of the blade, which was subject to various configurations in order to simulate different degrees of damage. Excitation was performed in two ways: near the delamination zone in a simulation of operational wind excitations, and with a bar designed to excite torsional modes of the wind turbine blade.

We compare the data collected from the wireless sensors against wired sensors to demonstrate their performance. We explore methods for determining damage. We first explore results of autoregressive coefficients for indicating damage levels. Finally, we demonstrate the use of damage sensitive features from the wavelet transforms of input and output signals to provide a method suitable for non-stationary blade excitations.

KEYWORDS : *Structural Health Monitoring, Damage Detection, Wind Turbine, Wireless sensing, Wavelets.*

INTRODUCTION

Detecting damage in wind turbine blades is a very important problem in structural health monitoring. The prevalence of wind power has grown immensely in recent years, and as the size and power of wind turbines grow, the cost of failures is likewise greater. As a result, the value of detecting ongoing and upcoming failures grows accordingly. This ultimately leads to a focus on wind turbine blades, which are the subject of the most common structural damage to turbines, are the costliest to repair, both in terms of time and budgetary resources. Furthermore, even minor damage to blades can progress to serious secondary damage to the entire wind turbine system.[1] Related problems involve determining loading on wind turbine blades, either for danger of impact, as in the case of ice forming on the blade surface, and/or damage to the structure incurred by other-than-anticipated loadings.

Remedies to such problems are addressed through new innovations in sensor technology. As sensors become cheaper, more ubiquitous, lower power, but more powerful and more capable of embedded algorithms, new methods of determining damage quickly on-site become more important. Practical aspects of deployment determine the feasibility of such sensors networks, with special import to wireless sensor networks that take advantage of the extra low-power abilities of Microelectromechanical systems (MEMS) to effect long-term deployments. In section one, we show a description of the test set-up including instrumentation and the iterations through variables altered. In section two, an application is applied for time-series analysis of the measurements. In section three, damage detection methods are attempted with wavelets.

1 DESCRIPTION OF TEST

1.1 Structure and Objectives

Testing took place September 2014 at DTU Risø Campus on a 34 meter wind turbine blade. The tip of the blade is cut off resulting in a blade length of 29 meters in order to fit the blade into the blade test facility. The blade was suspended in a cantilever state, fixed from the root, with the trailing and leading edges parallel with the ground. The blade itself was suspended off the ground between 2m and 20m, rising from the root.

The characteristics of the blade had been previously explored with Operational Modal Analysis (OMA), and the focus now turned to damage detection. The particular problem addressed was that of delamination--separation of layers of fiber composite layers in the lay-up of a wind turbine blade, especially at the edges. This is a very difficult failure mode to detect, in that it cannot be easily detected until the failure is obvious, and often catastrophic. [2] After OMA studies on the blade had been performed, a delaminated area had been cut into the trailing edge in stages, with new OMA testing in between each stage. A series of tests was performed that would yield a dataset that would be well-equipped to perform damage detection algorithms on several different damage states and other variables-- loading, as well as different sensor placements. A series of variables were defined that could be iterated through, as outlined in Table 1. The loading was applied locally near the delamination area with a muffled blunt instrument, in a simulation of local random loading as the region may experience in the field. The other type of excitation was a torsional application as applied to a torsion bar attached in one of two locations, depending on the iteration, also according to the table. The damage level was simulated in the test facility by a series of eleven bolts spaced evenly across the 1.2m delamination zone. Tightening all the bolts completely was the "undamaged" state, and loosening the bolts signaled the completely delaminated damage state.

Table 1: Variables iterated through in testing.

Variable	Description
Excitation	local excitation with hammer
Excitation	torsion bar
Damage	11/11 bolts tightened
Damage	9/11 bolts tightened
Damage	5/11 bolts tightened
Damage	2/11 bolts tightened
Damage	0/11 bolts tightened
Sensor Placement/Loading	sensor #123 in orientation A, torsion excitation at tip
Sensor Placement/Loading	Sensor #123 in orientation B,

	torsion excitation at tip
Sensor Placement/Loading	Sensor #123 in orientation c, torsion excitation at tip
Sensor Placement/Loading	Sensor #123 in orientation A, torsion excitation at 13.25m along blade

A combination of all conditions were performed in the lab, resulting in a total of 2*5*4 = 40 trials. The intention of compiling such a complete combination of all variables was to make it possible to isolate the damage states, as described in the application section of this paper. Each test consisted of two minutes of continuous excitation.

1.2 Set-Up

The orchestration of measurements was done in parallel in two different ways, both by a series of high-performance sensors, wired, by DTU, and a series of low-power wireless accelerometers by Stanford Researchers.

The set-up by DTU included 20 accelerometers placed along the perimeters of the blade, on the leading and trailing edge. The accelerometers connected via a wired connection, and were highly accurate, with noise less than 0.01 G . Accelerations were taken at a sampling rate of 4096 Hz, and were collected by a central unit, and immediately normalized. Other measurement devices included string potentiometers and direct displacement measures, but are not in the scope of this paper.

Figure 1: Sensor Placements for DTU Accelerometers

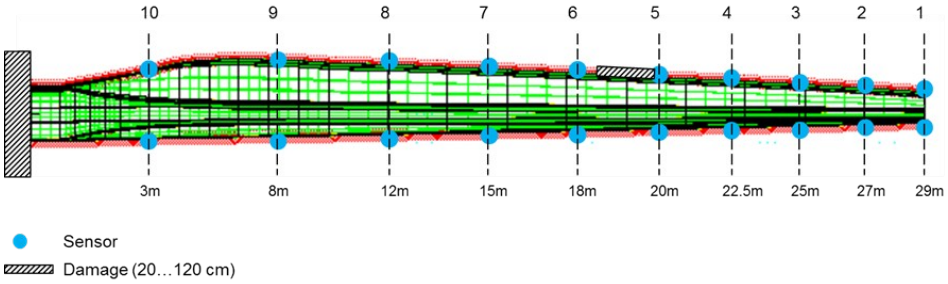

The set-up by Stanford researchers was four wireless accelerometers, in integrated units: plastic-bot. 4 inches. .6 pounds. The sensor system was developed out of a field of work demonstrating reliability of a simple single-hop implementation with Time Division Multiple Access (TDMA) [2], which was borne out by the results of the testing.

Though the sensor system was low-power and wireless, the communication reliability was extremely effective for the test: over 99.99% of packets were delivered successfully.

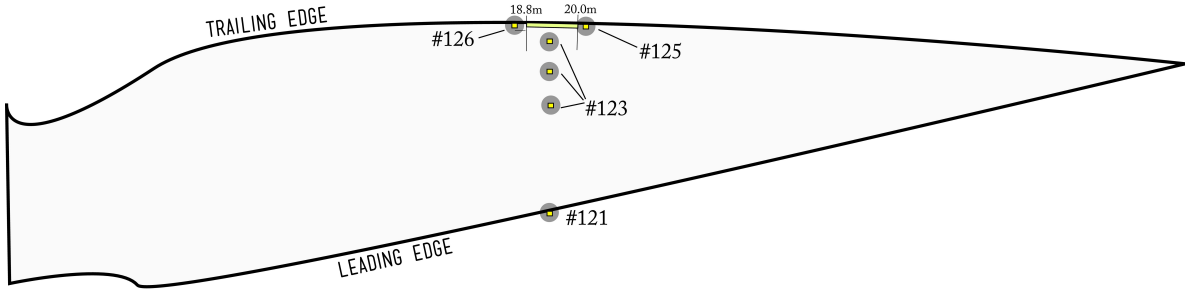

Figure 2: Sensor Placements for DTU Accelerometer+s

Table 2: List of location for Stanford instrumentation.

Sensor	Distance from Root (m)	Description
121	20.2m	On leading edge
125	20.0m	On trailing edge
126	18.6m	On trailing edge
123 (orientation A)	19.5m	On blade cap
123 (orientation B)	19.5m	55cm from trailing edge
123 (orientation C)	19.2m	11cm from trailing edge

2 APPLICATION: RELATING AUTOREGRESSIVE COEFFICIENTS TO DAMAGE LEVELS

Algorithms are explored to relate the space of data, for both the Stanford researchers' data as well as the data collected by the DTU instrumentation, involving time-series analysis. Autoregressive coefficients have been shown to correlate with stiffness when extracted from measurements developed from ambient vibrations, and combined[4]. There are many choices that are incurred when extracting autoregressive coefficients, such as the sampling frequency (which can vary from the sampling rate of the sensor, in that it can be downsampled to a lower frequency if desired); it is important to perform analyses on the proper frequency: a sampling rate over 3 times the desired frequency content to collect will require higher AR order to compensate. [5]

Before autoregressive coefficients were first calculated, a study was made of the time-series behavior of the acceleration measurements in order to gain an understanding of the ARMA model order. The correlation and partial correlation of the time series were examined to reveal the underlying time-series behavior: a report from one such run is shown in Figure 3. From the absence of the partial autocorrelation after lag 6, and the continuing behavior of the autocorrelation for further lags, damping gradually, the measurements appear to be consistent with a ARMA(6,1) time series: six autoregressive coefficients and a moving average of the last model. Comparisons of AR(6) vs ARMA(6,1) coefficients revealed similar results. The measurements are normalized to a zero-mean and standard-deviation of one before tests such that the level of loading should not make a difference in the correlations that result. The coefficients are drawn from “chunks”-- the measurement time history divided into multiple same-sized regions. The choice of the chunk size is ultimately one of calibration. The ARMA coefficients for each of the different instrumentations were likewise compared; one such comparison can be seen in Figure 4. The distribution of coefficients are typically in a Gaussian or Gaussian Mixture Model. Here, we see the first

autocorrelation coefficient, which for both set-ups for the same run yields similar results, the spread of the DTU measurements being slightly wider.

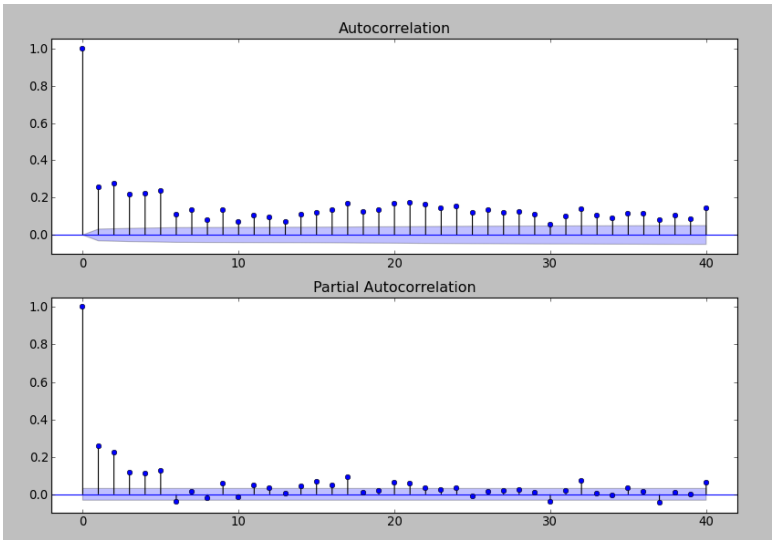

Figure 3: Autocorrelation and partial autocorrelation for acceleration time history

Exploring the entire space dictated by the variables and other calibration choices (chunk size, model order, downsampling) is done in part, though is intractable to brute force, owing to the large dimensionality and computational expense one incurs. The overall pattern of a comparison across any one variable (such as across the five damage states): the measurements are normalized and downsampled to be consistent with the sampling of the Stanford measurements (in the case of the DTU sensors, this is a downsampling of x30), AR is calculated and turned into a distribution, such as seen in Figure 4. The centroid of the distribution is extracted, and the space is explored in higher dimensions.

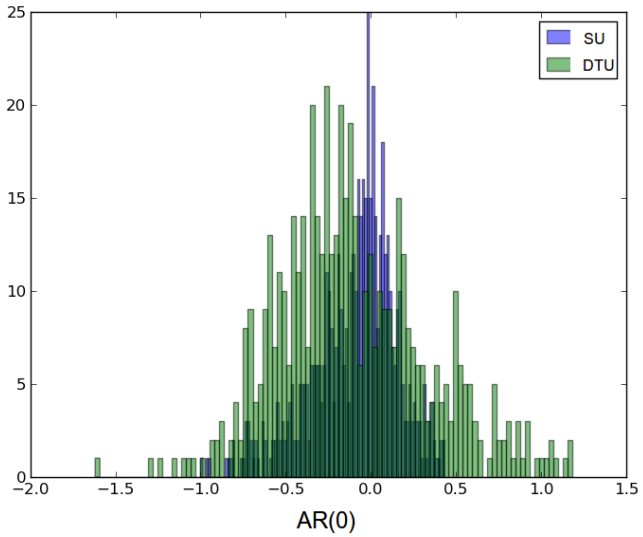

Figure 4: Comparison between sensor setups of first autoregressive coefficient distribution for all chunks for arbitrary run

Some patterns are seen to develop: the distance between the coefficients can be measured either in the space of any one. We see in Figure 5 two such comparisons. In (a), a variable that is easily distinguished, the type of loading local or torsional, and (b) the five damage states, in torsion loading condition (from tip). Loading is consistently easy to determine, whereas the damage is clustered together.

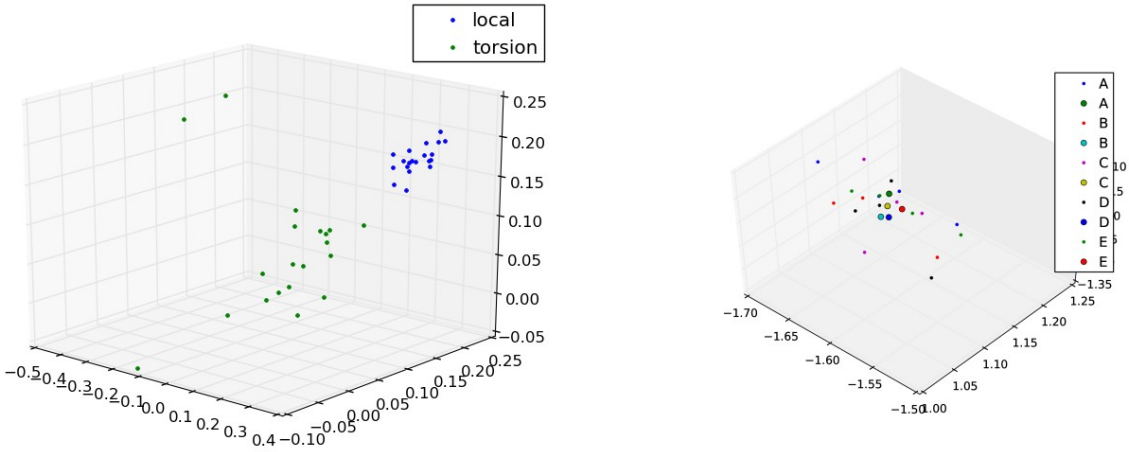

Figure 5: Comparison of AR(0) through AR(2) centroids for all chunks for (a) all runs, split by different loading variables (Stanford sensors) (b) All torsional runs, divided by Mean value of the input-output DSF per direction and sensor location for the torsional excitation

3 Application of Wavelet-based Damage Detection Algorithms

Two different damage detection algorithms are applied to the data collected by DTU. Both algorithms are based on the Continuous Wavelet Transform (CWT) of acceleration measurements and have been developed for earthquake damage detection in civil structures. The first algorithm, proposed by Balafas and Kiremidjian [6] requires both an input (excitation) and an output (response) signal. Given the array of sensors, the algorithm was applied to pairs of adjacent sensors, with the “input” being the sensor that is closer to the root of the blade and the “output”' being the sensor that is closer to the tip of the blade. The second algorithm, proposed by Noh [7] does not require an input signal but requires knowledge of the fundamental frequency of the structure. In the present analysis, the fundamental frequency is estimated by the frequency with the highest Fourier amplitude. Detailed presentations and derivations of the algorithms and the resulting Damage Sensitive Features (DSFs) can be found in the respective references. Due to the size of each recording (approximately 2 minutes at 4096 Hz), the data was downsampled by a factor of 3 and split into signals of approximately 750 points each. This way, a vector of DSF values was obtained for each recording, rather than a single value. For clarity of notation, the algorithm proposed in [6] will be referred to as “input-output” algorithm, while the algorithm proposed in [7] will be referred to as “output-only” algorithm. The results for the third feature proposed in the input-output algorithm and the first feature proposed in the output-only algorithm are presented.

The vector of DSF values for the input-output algorithm was calculated for each sensor pair and sensor axis. The mean of the DSF vector is assigned as the DSF value for each sensor location and direction. The sensor location is the location of the sensor considered as the ``output'' signal. The mean DSF value is then calculated for the leading and trailing edges, each sensor axis (direction) and each sensor location and plotted in Figure 6. The hammer excitation did not exhibit any trend

with increasing damage and only the torsional excitation is presented. While there were five different damage levels, only the lowest and highest are plotted as the algorithm could not detect smaller increments in damage. It can be observed from Figure 6 that the mean DSF increases in the edge direction and the leading edge. Furthermore, the highest increase can be observed in locations 5 and 6, which is also the location of the delamination. The increase of the DSF in the trailing edge, where there is no damage, is not significant. In the gravity direction, there is an increase in most locations and both edges but no damage localization can be observed.

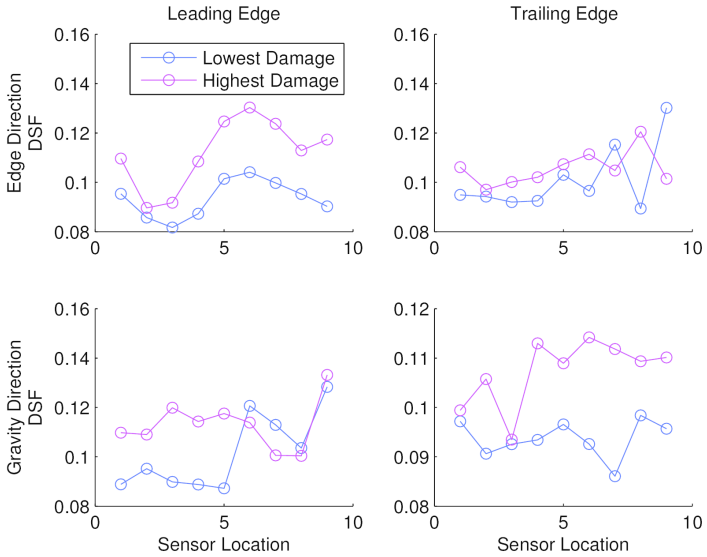

Figure 6: Mean value of the input-output DSF per direction and sensor location for the torsional excitation

The same procedure was followed for the output-only algorithm. In this case, the DSF vector and mean value for each location was the value calculated from the signal of the respective sensor. Figure 7 plots the mean DSF of all recordings for each sensor location and the torsional excitation. In this case, the gravity direction appears more informative for the location of damage; the DSF in the leading edge increases while the DSF in the trailing edge does not increase significantly. Furthermore, the highest increase in DSF in the leading edge appears to be in the location of damage. The edge direction, however, exhibits and increase in DSF in both the leading and trailing edge, possibly indicating damage, but does not provide any further insight in the specific location of damage.

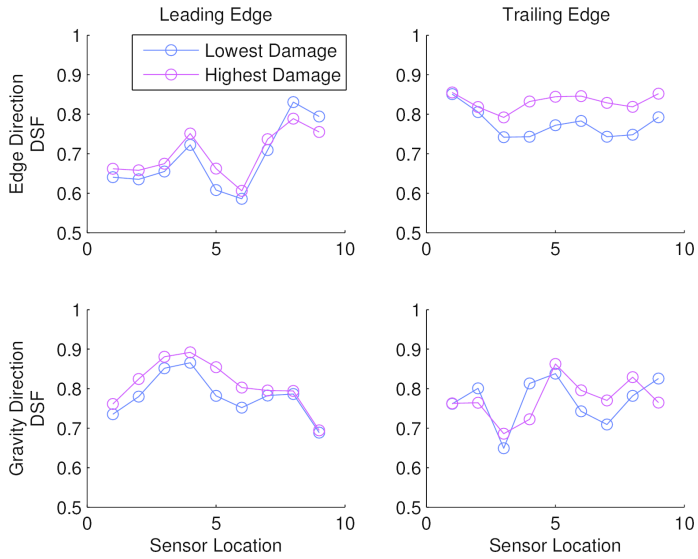

Figure 7: Mean value of the output-only DSF per direction and sensor location for the local excitation

It should be noted that the recordings from both excitations and the distributions of the DSF values, rather than just their means, were investigated. However, there was no clear trend in these cases and the results are not presented.

CONCLUSION

The results demonstrate a framework for using low-power wireless accelerometers for operational damage detection on full-scale wind turbine blades. In particular, we demonstrate a reliable and robust wireless sensor system that is a first step towards a cost effective practical field deployment system. A demonstration of applications for the data are shown for analyzing the data using time-series autoregressive and wavelet-based methods.

REFERENCES

[1] C.C. Ciang, J.R. Lee, H.J. Bang. Structural Health Monitoring for a Wind Turbine System: a Review of Damage Detection Methods, *Measurement Science and Technology*, 19: 12, 2008.

[2] A. Jüngert. Damage Detection in wind turbine blades using two different acoustic techniques. *The NDT Database & Journal (NDT)*, 2008

[3] R. Bajwa, R. Rajagaopal, P. Varaiya, R. Kavaler. In-pavement Wireless Sensor Network for Vehicle Classification. *Proc. IEEE ISPN '11*, IEEE: 85-96, April 2011.

[4] K. K. Nair, A. S. Kiremidjian, K.H. Law. Time series-based damage detection and localization algorithm with application to the ASCE benchmark structure, *Journal of Sound and Vibration,* 291(1): 349-368, 2006.

[5] M. Smail, M. Thomas, A. Lakis. ARMA models for modal analysis: effect of model orders and sampling frequency, *Mechanical Systems and Signal Processing*, 13(6):925-941, 1999.

[6] K. Balafas, A.S. Kiremidjian. Extraction of a series of novel damage sensitive features derived from the continuous wavelet transform of input and output acceleration measurements, *Proc. SPIE 9061, Sensors and Smart Structures Technologies for Civil, Mechanical, and Aerospace Systems 2014*, March 2014.

[7] H.Y. Noh, K.K. Nair, D.G. Lignos, A.S. Kiremidjian. Use of Wavelet-Based Damage-Sensitive Features for Structural Damage Diagnosis Using Strong Motion Data, *Journal of Structural Engineering*, 137:1215-1228, October 2011.